Taylor & Francis
Taylor & Francis Group

RESEARCH ARTICLE

🔓 OPEN ACCESS   Check for updates

Dendritic cell derived exosomes loaded with immunoregulatory cargo reprogram local immune responses and inhibit degenerative bone disease *in vivo*

Mahmoud Elashiry 🄳[a], Mohamed M. Elashiry[b], Ranya Elsayed[c], Mythily Rajendran[c], Carol Auersvald[c], Rana Zeitoun[d], Mohammad H. Rashid[e], Roxan Ara[e], Mohamed M. Meghil[a], Yutao Liu[f], Ali S. Arbab[e], Roger M. Arce[g], Mark Hamrick[f], Mohammed Elsalanty[h], Marshall Brendan[f], Rafal Pacholczyk[i] and Christopher W. Cutler 🄳[c]

[a]Department of Periodontics, Department of Oral Biology and Diagnostic Sciences, Dental College of Georgia at Augusta University, Augusta, GA, USA; [b]Department of Periodontics, Dental College of Georgia at Augusta University, GA, USA, Department of Endodontics, Faculty of Dentistry, Ain Shams University, Cairo, Egypt; [c]Department of Periodontics, Dental College of Georgia at Augusta University, GA, USA; [d]Department of Oral Biology and Diagnostic Sciences, Dental College of Georgia at Augusta University, Department of Fixed Prosthodontics, Faculty of Dentistry, Ain Shams University, Cairo, Egypt; [e]Department of Biochemistry & Molecular Biology, Georgia Cancer Center, Augusta, GA, USA; [f]Department of Cellular Biology and Anatomy, Medical College of Georgia at Augusta University, GA, USA; [g]Department of Periodontics and Oral Hygiene, School of Dentistry, The University of Texas Health Science Center at Houston, Houston, TX, USA; [h]Medical Anatomical Sciences, College of Osteopathic Medicine of the Pacific, Western University of Health Sciences, Pomona, CA, USA; [i]Georgia Cancer Center, Augusta, GA, USA

ABSTRACT

Chronic bone degenerative diseases represent a major threat to the health and well-being of the population, particularly those with advanced age. This study isolated exosomes (EXO), natural nano-particles, from dendritic cells, the "directors" of the immune response, to examine the immunobiology of DC EXO in mice, and their ability to reprogram immune cells responsible for experimental alveolar bone loss *in vivo*. Distinct DC EXO subtypes including immune-regulatory (regDC EXO), loaded with TGFB1 and IL10 after purification, along with immune stimulatory (stimDC EXO) and immune "null" immature (iDCs EXO) unmodified after purification, were delivered via I.V. route or locally into the soft tissues overlying the alveolar bone. Locally administrated regDC EXO showed high affinity for inflamed sites, and were taken up by both DCs and T cells *in situ*. RegDC EXO-encapsulated immunoregulatory cargo (TGFB1 and IL10) was protected from proteolytic degradation. Moreover, maturation of recipient DCs and induction of Th17 effectors was suppressed by regDC EXO, while T-regulatory cell recruitment was promoted, resulting in inhibition of bone resorptive cytokines and reduction in osteoclastic bone loss. This work is the first demonstration of DC exosome-based therapy for a degenerative alveolar bone disease and provides the basis for a novel treatment strategy.

Introduction

Periodontitis (PD) is a chronic bone disease that affects over 50% of the U.S. population [1]. PD has been linked to increased risk of a number of other diseases with more serious mortality and morbidity profiles [2,3]. Histopathological studies of PD lesions implicate neutrophils as the first line of defence, which eventually turn against the host [4]. Severe PD lesions are infiltrated with B cells, macrophages and dendritic cell (DC) clusters with CD4+T cells [5–8], the equivalent of ectopic lymphoid follicles [9,10].

The immune response can be shaped based on the maturation status of DCs [11]. Immature DCs (iDCs)

can promote immune tolerance by induction of T cell anergy and regulatory T cell (Treg) response to terminate inflammation [12–17]. Whilst mature DCs can direct a T-helper cell 17 (Th17) response to eradicate invading bacteria. Th17 effector T cells appear to play a bone degenerative role [13,18,19], while Tregs reportedly attenuate inflammatory bone loss [20,21]. Restoration of Treg stability in PD patients by implementation of an anti-infective protocol correlates closely with clinical improvement [22], but as yet no effective immunomodulatory agent for PD has been identified.

The marked ability of DCs to direct the immune response has led to use of whole DCs, modified to be

Table 1. Cytokine and DCs maturation marker CD86 profile in DCs derived exosomes subsets.

	regDCs exo	iDCs EXO	stimDCs EXO
TGFB1	+	-	-
IL10	+	-	-
IL6	-	-	+
TNF	-	-	+
IL1B	-	-	+
CD86	-	+	++

+ Detectable
- Below Detectable limit

tolerogenic genetically or with immunosuppressive cytokines, to suppress inflammatory disease in animals. However, immunomodulation using DCs or other immunosuppressive cells like Treg has some limitations, including rarity and phenotypic instability of whole cells *in vivo* [23].

Targeting proinflammatory cytokines using inhibitors of TNF and IL1B has shown therapeutic efficacy for treating inflammatory diseases. However, effects are short lived due to rapid clearance and proteolytic degradation in challenging inflammatory environment [24].

Extracellular vesicles (EV) of endosomal origin, called exosomes (EXO), can be isolated from DCs, and their small size (30–150nm) can optimize the delivery of this cargo to recipient cells. Moreover, DC EXO harbour unique proteins that shield them from attack by the complement system [25] and promote binding to tissue integrins [26]. DC EXO can also be loaded with cytokines or peptides using direct or indirect approaches [27–29]. Immunostimulatory cargo-loaded mature DCs EXO have been touted for anti-cancer benefits [30], while tolerogenic DC-derived EXO equipped with immunoregulatory cargo offer promise for treatment of autoimmune and inflammatory diseases [31].

The goal of the current study was to characterise the immunobiology of DC EXO subtypes in vitro and in vivo and their ability to reprogram immune cells responsible for inflammatory bone loss. After purification, reg DC EXO were loaded with immuno-regulatory cytokines TGFB1 and IL10. These cytokines appeared localized on the EXO transmembrane domain and within the EXO lumen, where they were protected from proteolytic degradation. Both *in vitro* and in vivo studies show important role for EXO-encapsulated TGFβ and IL-10 in prevention of DC maturation; moreover, TGFβ1 was required for increased induction of CD25+Foxp3+T cells (Treg). Moreover, regDC EXO inhibited Th17 and decreased

bone loss, further evidenced by decrease in Trap+ osteoclasts.

We conclude that DC EXO loaded with molecular cargo to modulate Th17/Treg balance is an effective immunotherapeutic approach to regulate degenerative bone disease *in vivo* in this model.

Material and methods

Ethics statement

The Institutional Animal Care and Use Committee (IACUC) of Augusta University (protocol # 2013–0586) approved all experimental procedures.

Generation and culture of iDCs, regDCs and stimDCs

Bone marrow was isolated from tibias and femurs of 6 – to 8-week-old mice as previously described [32]. ACK cell lysing buffer was used to lyse contaminating erythrocytes (Invitrogen, Thermofisher scientific, and Columbia, SC, USA). Cells were cultured for 24 h in complete media (RPMI 1640 containing 10% FBS and 100 IU/mL penicillin/streptomycin) to remove adherent macrophages. Non-adherent cells were then cultured in growth media, containing 20ng/ml of murine GM-CSF and IL-4 (Peprotech, Rocky Hill, NJ, USA). Culture media was changed every 2days and cells were harvested on day 6 and incubated for 2days in EXO depleted complete media (by using EXO free FBS) to generate iDCs. To generate stimDCs, part of the harvested cells were cultured in fresh EXO depleted complete medium containing 1ug/ml LPS (Sigma, St. Louis, M. O., USA) for 48h, and cells were harvested on day 8. To generate regDCs, DCs were cultured for 4days and harvested on day 5 for TGFB1/IL10 recombinant cytokines treatment in which, 1×10^7 DCs were incubated for 2hours with 1ug/ml TGFB1 (R&D Systems, Inc. Minneapolis, MN) and 1μg/mL of the recombinant murine IL-10 (Cell Sciences, Canton, Massachusetts) in total volume of 1mL serum-free media, then diluted 1:10 in fresh complete media for further incubation. On day 6, regDCs were harvested, washed and cultured for 48h in EXO depleted growth media and isolated on day 8. On day 8, culture supernatants were collected for EXO purification. Cultured iDCs, regDCs and stimDCs were defined by expression level of CD11c+ (N418) (Invitrogen), MHCII (M5/114.15.2) (Milteny biotech Auburn, CA,USA) and CD86 (GL1) (Invitrogen), by flow cytometry (Milteny biotech) and by level of pro/anti-inflammatory cytokine mRNA by

PCR, including IL6 (Mm00446190_m1), IL12 (Mm01288989_m1), IL23 (Mm00518984_m1), TGFB1: Mm01178820_m1 and TNF: Mm00443258_m1, (Thermofisher Scientific).

EXO isolation, purification and cytokine loading of regDC EXO

EXO isolation was performed as previously described [24]. Briefly, the DC culture supernatants was subjected to three successive centrifugations at 500g for (5 min), 2000g for (20 min), and 10,000g for (30 min) to eliminate cells and debris, followed by ultrafiltration 3× with 0.2 um and 3× with 100 kDA filters (to remove free proteins) and ultracentrifugation for 1.5h at 120,000g. To further remove excess free proteins, EXO pellets were washed with a large volume of PBS and ultra-centrifuged 2× at 120,000g for 1.5h, and finally re-suspended in 100 ul of PBS for further studies. In the case of regDC EXO, 1×10^9 particles were additionally actively loaded by sonication [27] with 5ug TGFB1 and 5 ug IL10 in 500 ul of PBS then filtered 3x by ultrafiltration with 100KDA filter to remove free proteins and washed 3× with large volume of PBS and ultra-centrifugation at 120,000g for 1.5h to further purify EXO from free molecules, and finally re-suspended in 100 ul of PBS. Supernatant of which regDCs EXO were suspended was isolated and checked for any contaminants by ELISA. The integrity of EXO proteins and loaded cytokines was assessed after sonication using Western blot analysis (Fig. S1A). The size and zeta potential of sonicated exosomes was measured using Nano particle tracking analysis (Fig. S1B). EXO subtypes were quantified by nano-tracking analysis and a BCA protein assay. The yield of exosomes from their respective DC subtypes are as follows:

RegDCs EXO: approximately four vesicles per one cell per hour

ImDCs EXO: approximately five vesicles per one cell per hour

StimDCs EXO: approximately eight vesicles per one cell per hour

Characterization of DC-Derived EXO

Western blotting

EXO lysates were extracted to determine EXO markers and pro/anti-inflammatory cytokines by Western blotting analysis using anti-TSG101 (MA1-23,296), anti-Alix (MA1-83,977), anti-CD63 (10628D) and GRP94 (MA3-016) from (Invitrogen, Thermofisher scientific West Columbia, SC, USA), anti-MHCII (MABF33) from (Sigma, St. Louis, M.O.,USA), anti-IL1B

(63,124), anti-TNF (11,948), anti-iL6 anti-TGFB1 (3711) and anti-B-Actin (3700) from (Cell Signaling Technology, Danvers, MA, USA) and CD86 (AF-441-NA) and anti-IL10(MAB417) from (R&D Systems, Inc. Minneapolis, MN, USA)

Electron microscopy

As described previously [33] EXO samples were loaded onto a copper grid. After precipitation of EXO, the sample liquid was extracted and counter stained with 2% phosphotungstic acid solution for 10min then placed under an incandescent lamp for 5 min. EXO sample was examined with TEM. Immune gold plating was done using anti-CD63, anti-TGFB1 and anti-IL10 primary antibodies.

Nanoparticle tracking analysis

Nanoparticle tracking analysis (NTA) was used to visualize and quantitate size and count of nanoparticles in suspension. Briefly, as described previously [33–36], 10 ul of EXO suspension was loaded into the sample chamber of ZetaView PMX 110 (Particle Metrix, Meerbusch, Germany). Data analysis was performed with software (ZetaView 8.02.28).

EXO miRNA microarrays

miRNAs were isolated from EXO using Total EXO RNA Kit (4,478,545, Thermofisher Scientific) according to manufacturer's protocol. The concentration of miRNA was determined using a NanoDrop spectrophotometer (Thermo Scientific) and the quality of miRNA analysed using an Agilent 2100 Bioanalyzer. Analysis of miRNAs was performed using an Affymetrix GeneChip® miRNA 4.0 Array at the Integrated Genomics Core, Augusta University, GA. The P-value cut-off of 0.05 and the miRNAs with a fold change above 1.5 were considered differentially expressed. Bioinformatic analysis was performed using Ingenuity Pathway Analysis (IPA), and TargetScan software was used to identify computationally predicted miRNA-mRNA target relationships [37].

ELISA

EXO lysed with ELISA lysis buffer (#7018, Cell signaling) or intact were suspended in PBS and analysed according to the manufacturer, using ELISA kits for TGFB1 (BMS608-4) and IL10 (BMS614INS) both from (Invitrogen, Thermofisher scientific West Columbia, SC, USA)

EXO resistance to proteolytic digestion assay

RegDCs EXO and Free TGFB1 and IL10 with equivalent concentration to those loaded to regDCs EXO were divided to trypsin or proteinase k treated at 37°

C with concentration of 25µg/ml for 60min and non-treated groups and subjected to Western blotting for TGFB1 and IL10 detection.

T-cell isolation

CD4+ T cells were isolated from mice spleens using negative selection with Mouse T-cell Enrichment Kit (#19,765) (Stem cell technologies, Cambridge, MA, USA). T-cell purity was assessed by flow cytometry analysis of CD4, CD3 and CD8 markers and were typically >95% pure.

EXO uptake invitro

For EXO uptake study *in vitro*, EXO labelled with Dil (D282, Thermofisher Scientific) were co-cultured with DCs or CD4+T cells for 24h. Cells were fixed and stained on glass slides with phalloidin (A12379) and DAPI (D1306) (Invitrogen, Thermofisher scientific West Columbia, SC, USA). The images were obtained by scanning confocal fluorescence microscopy.

Immune modulatory effect of EXO in vitro

DCs activation: The immune modulatory influence of EXO subtypes on acceptor DC was investigated by incubating 10^8/ml EXO in DC culture on day 5, followed by harvesting on day 8 and measuring the expression of antigen presenting and maturation markers MHCII and CD86 by flow cytometry and mRNA level of proinflammatory cytokines including IL6, IL12 and IL23. Analyses were performed in the presence or absence of DC stimulators/inhibitors including LPS and neutralizing antibodies against TGFB1 (MAB1835, R and D) and IL10 (JES5-2A5, Thermo fisher scientific). Phosphorylation of TGB1 and IL10 transcription factors and MHCII was assessed by Western blot using anti PSMAD2/3 (D6G10), anti SMAD2/3 (D7G7), anti PSTAT3 (D3A7), antiSTAT3 (D3Z2G) and MHCII (MABF33) antibodies and GAPDH (D16H11) (Cell Signaling Technology, Danvers, MA, USA).

Antigen-presentation

T-cells specific for OVA antigen peptides were isolated from spleen of OT-II transgenic mice and stained with carboxyfluoresceine succinimydil ester (CFSE) (C1157, Thermo fisher scientific) followed by washing to remove excess free CFSE . 10^8/ml treated – (EXO added to DCs culture on day 5) or untreated (control) – DCs were incubated with OVA peptide (O1641, Sigma Aldrich) 1µg/ml for 24hours, then washed and co-cultured with CD4+T-cells, at a ratio of 1:10 DCs to T-cells in a 96 well round bottom plate and complete RPMI 1640, and incubated at 37° and 5% CO2 for 5days. T-cell proliferation was assessed by % loss of CFSE in each generation by flow cytometry.

T-cell activation and differentiation

To stimulate Tregs or effector CD4+ T-cell proliferation, 96 round-bottom plate were coated and incubated overnight at 4° with 10µg/ml anti CD3 antibody. CFSE-stained T-cells were added with or without EXO 10^8/ml to the plate in complete RPMI 1640 media containing 10µg/ml anti CD28 antibody and incubated at 37° and 5% CO2 for 5days. In some experiments, TGFB1 and IL10 neutralizing antibodies were added. T-cell proliferation was assessed by CFSE dilution using flowcytometry analysis by gating on the CD4+ cells. Regulatory T-cells (Tregs) were identified by gating on double positive cells for FOXP3 (FJK-16s, Thermo fisher Scientific) and CD25 (PC61.5, Thermo fisher Scientific), in CD4+ (GK1.5, Thermo fisher Scientific), population while T-helper 17 induction was identified by measuring IL17 median fluorescent intensity in CD4 population by using anti IL7 Antibody (eBio17B7, Thermofisher scientific), followed by flow cytometry. Supernatants were analysed for IL17 by ELISA (BMS6001, Thermo fisher Scientific). Western blot was used to assess the expression of FOXP3 using antiFOXP3 (FJK-16s, Thermo fisher Scientific).

In vivo imaging of EXO biodistribution in murine periodontitis model

Induction of experimental periodontitis (PD) in mice model

This model was developed by ligation of the upper right second molar with black silk suture to accumulate bacteria and induce inflammation induced alveolar bone loss as described previously [38,39]. This model does not induce inflammatory bone loss in germ free animals and is thus dependent on the endogenous flora.

In vivo imaging: 1.5 to 2 mCi of Indium-111-oxine (AnazaoHealth Corporation, Tampa, FL, USA) in PBS was added to 200µl of exosomes particles ($\sim 2 \times 10^9$ particles) and incubated at 37°C for 20minutes. Free indium was removed by repeated PBS washes through an Amicon ultrafiltration device. Collected In-111-labelled EXO were diluted to 200 µCi of radioactivity per dose and injected intravenously in tail vein or locally in palatal tissue in periodontitis mice model on day 3 relative to ligature placement. Control

animals received injection of equivalent activity of free Indium-111-oxine. Whole body and head single photon emission spectroscopy (SPECT) images were acquired by Mediso's nanoScan microSPECT/CT system ((Mediso, USA) at 24hours after injection, and images were reconstructed to determine radioactivity in maxilla and whole body. Radioactivity in maxilla was expressed in percent of activity in the whole body (total radioactivity). Maxilla were excised and *ex vivo* radioactivity measurements were performed by gamma counter (Perkin-Elmer Packard Cobra II Auto-Gamma) [40].

EXO uptake in vivo in murine periodontitis models

For EXO uptake *in vivo*, Dil-labelled EXO were locally injected through palatal gingiva on day 3 relative to ligature placement. After 24 hrs, mice were sacrificed and gingival tissues from maxilla were removed and treated with Collagenase type II (2mg/mL) and DNase I (1mg/mL) (both from Sigma Aldrich) solution in PBS plus 2% FCS for 30min at 37°C in a shaker bath. 0. 25µL of 0.5M EDTA per 2mL sample were added and incubated for an additional 15minutes, followed by centrifugation at 4°C, $400 \times g$ for 8min in PBS with 2% FBS. Supernatants were removed, cells were suspended in PBS with 2% FBS and filtered through a 70-µm cell strainer and stained on glass slide with primary antibodies including antiCD11c (N418), antiCD4 (GK1.5) and Secondary antibodies including Goat anti-Rat IgG, DyLight 488 (SA5-10,018) and Goat anti-Hamster IgG, Alexa Fluor 488 (A-21,110), all from thermofisher Scientific. Then slides were mounted with DAPI and images were captured by scanning confocal fluorescence microscopy.

Immune modulatory effect of EXO in vivo

The immunomodulatory functions of EXO in six experimental groups were analysed. **Group 1** received locally 10 ul of phosphate buffer saline (PBS) (n=5). The other five groups of animals were subjected to ligation with 5–0 silk to the upper left second molar to induce inflammatory bone loss. The contralateral molar tooth in each mouse was left un-ligated to serve as baseline control for alveolar bone volume measurements. The ligatures remained in place in all mice throughout the experimental period (nine days). **Group 2** received ligation plus local administration of 10 ul of PBS (n=5), **Group 3** received ligation plus local delivery of 10^8 particles of regDCs EXO suspended in 10 ul PBS (n=5), **Group 4** received ligation plus local delivery of 10^8 particles of iDCs EXO suspended in 10 ul PBS (n=5), **group 5** received ligation plus local delivery of 10^8 particles of

stimDCs EXO suspended in 10 ul PBS (n=5), and **group 6** received ligation plus 60 ng TGFB1 and 10 ng IL10 which are equivalent concentrations to TGFB1 and IL10 in regDCs EXO as determined by ELISA. The delivery of control PBS or EXO in all groups was performed at days −2, 0 and 2 relative to ligature placement. After 9days of ligature placement maxilla and gingival tissue were harvested, and gingival cells were isolated. Cells were stained with antibodies against CD3 (17A2), CD86 (GL1), CD11c (N418), CD25 (PC61.5),CD4 (GK1.5),Foxp3: (FJK-16s), IL17A (eBio17B7), all from Thermofisher Scientific and MHCII (M5/114.15.2, Milteny biotech), in order to identify DCs and their activation markers and T cells subsets infiltrating gingival tissue. Draining lymph nodes were excised and cells were isolated and stained with anti-CD4 antibody to determine frequency of CD4+T cells by flow cytometry.

Immunohistochemical (IHC) staining of gingival tissue

Tissue blocks were de-paraffinized, cut into 5 µ sections and mounted on slides. Antigen retrieval was done in water bath heating with citrate buffer PH6. IHC staining with DAB/peroxidase was performed using the following antibodies against the proteins indicated: MHCII (ab180779, Abcam, Cambridge, MA), CD86 (GL1), FOXP3 (FJK-16s), IL17 (PA5-79,470), RANKL (PA5-87,147), all from Thermofisher Scientific and TNF (SAB4502982, Sigma Aldrich). Multiple random microphotographs were taken for each gingival tissue in lamina propria region, at 40× objective lens using Zeiss microscope (Zeiss AxioIma, Carl Zeiss Microscopy GmbH, Jena, Germany). Image-J software was used and a threshold was adjusted based on the negative control.

Micro-CT imaging and bone parameter analysis

Micro-CT imaging of maxillae was performed using a SkyScan 1272 microfocus X-ray system (SkyScan®, Kontich, Belgium) with software including NRecon reconstruction®, CTAn 1.8®, and CTvol. In this study, the X-ray source set at 70 kV and 100µA with the pixel size of 6µm, a 0.5-mm filter, and a tomographic rotation of 180° (rotation step of 0.2°). Residual bone volume (BV, µm3) around second upper molars was quantified and 3-D models were generated with teeth auto traced in yellow while bone in white [39,41].

Periodontal tissue histology

Formalin-fixed maxillae specimens were decalcified with EDTA and embedded in paraffin. Sections were

stained with haematoxylin and eosin, to evaluate alveolar bone loss at microscopic level.

Tartrate-resistant acid phosphatase staining (TRAP)

As described previously [42], TRAP staining for periodontal tissue sections used Acid Phosphatase, Leukocyte (TRAP) Kit (387A-1KT, Sigma Aldrich) to quantify osteoclastic cells, revealed by light microscopy. Multinucleated osteoclasts in interproximal bone and furcation were counted blindly and osteoclast density was expressed as number of osteoclasts per square micrometre of bone using computer software (ImageJ) [42].

In vitro osteoclastogenesis assay

1×10^5 EXO were co-cultured with murine CD4T cells in osteoassay 96 well plates (CLS3988, Sigma Aldrich) with 1×10^5 bone marrow cells and supplemented with 50ng/ml of RANKL (ab129136, Cambridge, MA) and 50ng/ml M-CSF (315–03, Rocky Hill, NJ, USA). The culture media was changed every 2days. On day 5 TRAP staining was performed to detect multinucleated osteoclasts using Acid Phosphatase Leukocyte (TRAP) Kit (387A-1KT, Sigma Aldrich).

Flow cytometry and antibodies

Staining was performed on ice, with Flow Cytometry Staining Buffer (Thermofisher scientific). Blocking of FC receptors (FCR) was achieved with mouse FcR blocking reagent (Miltenyi Biotec) for 15minutes on ice and protected from light, followed by addition of fluorophore conjugated antibody at recommended concentration on ice for 30minutes, after which cells were washed, re-suspended in flow cytometry buffer and data was acquired using Milteny biotech machine and software.

Real time PCR

Total RNA was isolated from DCs *in vitro* and from gingival tissue of the experimental groups used for *in vivo* studies using QIAGEN RNeasy mini kit (Qiagen, Inc., Valencia, CA, and USA). RNA concentration and purity were assessed with Nanodrop (NanoDrop 1000 UV-VIS Spectrophotometer Software Ver.3.8.1, Thermofisher Scientific). Ratio of 260/280 of 2.0 was deemed acceptable for further analysis, and was reverse transcribed to cDNA. Amplification by PCR was performed using the High-Capacity cDNA Reverse Transcription Kit and PCR in

total reaction of 20μL. Quantitative real-time PCR was performed using TaqMan gene expression primers specific for IL6 (Mm00446190_m1), IL12 (Mm01288989_m1), IL23 (Mm00518984_m1), TGFB1 (Mm01178820_m1) and TNF (Mm00443258_m1) IL10(Mm01288386_m1), FOXP3 (Mm00475162_m1), CTLA4 (Mm00486849_m1), Rankl (Mm00441906_m1) and Beta Actin (Mm02619580_g1), all from Thermofisher Scientific. RT-PCR was run in StepOnePlus Real-Time PCR System. Relative gene expression was calculated using delta-delta CT and plotted as relative fold change.

Western blotting

Cells or EXO lysates were extracted by addition of RIPA buffer supplemented by protease/phosphatase inhibitor cocktail and incubation for 20minutes on ice. Proteins (10μg) were separated using 14% Mini-PROTEAN TGX Precast Protein Gel (Bio-Rad Laboratories, Hercules, CA), and transferred onto PVDF membranes (Sigma-Aldrich). After blocking with 5% non-fat dry milk in PBS, the membrane was incubated with primary antibodies, washed with TBST and incubated with HRP-conjugated secondary antibodies for 1 h at room temperature. The membranes were developed using ECL kit and imaged using ChemiDoc MP Imaging Gel (Bio-Rad Laboratories, Hercules, CA).

Statistical analysis

Data analysis was performed by one-way ANOVA followed by Tukey's multiple-comparisons test or student T-test using GraphPad Prism 6 (GraphPad Software, La Jolla, CA). Values are expressed as mean ± standard deviation (SD) and experiments were done in triplicates.

Results

Generation and characterization of DC EXO subtypes prior to *in vitro* and *in vivo* functional testing.

EXO donor DC subtypes including immunoregulatory DCs (regDCs), immature DCs (iDCs), and immunostimulatory (stimDCs) were generated from bone marrow derived non-adherent cells of C57BL/6 mice, and phenotype and cytokine profiles characterized as follows: regDCs:CD11c +, low MHCII+, low CD86+, low CD80 +and low CD40+, iDCs: CD11c+, intermediate MHCII+, intermediate CD86+, intermediate CD80+, intermediate IL6+, intermediate IL12+and intermediate IL23+and stimDCs: CD11c+, high MHCII+, high CD86+, high

CD80+, high IL6+, high IL12+and high IL23+. From these DC subtypes, EXO were purified, quantitated and correct size distribution (30–150nm) confirmed by nanoparticle tracking analysis (Figure 1A). Further characterization indicates predominant population of EXO, as determined by immunogold-CD63 TEM (Figure 1B), immunoblot for Tsg101 (component of Escort1 complex), CD81, B-actin, Alix (Escort Associated Protein) and EXO negative marker GRP94 (Figure 1C), as previously reported [43].

Additional active loading by sonication of regDC EXO with TGFB1 and IL10 was achieved, residual proteins removed by further processing, and all DCs EXO subtypes analysed by immunoblot (Figure 1C) and ELISA (Figure 1D) revealing distinct molecular content of EXO subtypes as follows:regDCs (high TGFB1/IL-10, undetectable IL-6/TNF/IL-1B and CD86), iDCs (undetectable TGFB1/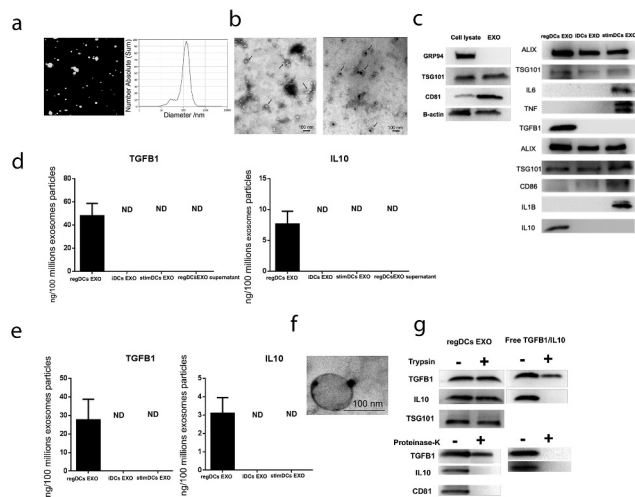IL-10, IL-6/TNF/IL-1B, low CD86) and stimDCs (undetectable TGFB1/IL-10, high IL-6/TNF/IL-1B and CD86) (Table. S1). The relative levels of TGFB1 and IL-10 in both lumen and transmembrane domain of regDC EXO was determined as in materials and methods, and as shown in (Figure 1D and Figure 1E). Neither TGFB1 nor IL10 were detectable in iDC EXO and stimDC EXO, nor in the PBS supernatant of regDC EXO after isolation, ruling out soluble carry over. Higher magnification TEM of regDC EXO confirms ELISA data, with TGFB1 inside and attached to outer EXO membrane (Figure 1F). Sonication of the exosomes did not affect the stability of exosomal protein markers such as Alix, TSG101 and tetraspanin CD81 as shown by Western blot analysis (Fig. S1A). Furthermore, the sonication did not influence the size or zeta potential of regDCs EXO as shown in Fig. S1B

Trypsin treatment of regDC EXO or free TGFB1/IL10 with concentrations equivalent to those loaded to regDC EXO confirmed protection of cytokines from proteolytic degradation by encapsulation in EXO as shown by Western blotting (Figure 1G). To further examine the resistance of regDCs EXO to proteolytic degradation, proteinase-k was used, which is a more potent protease . Proteinase-K treatment showed complete degradation of the free TGFB1 and IL10 and surface EXO proteins like tetrasapanin CD81 and IL10 in regDCs EXO while TGFB1 was partially degraded suggesting protection by EXO (Figure 1G). Biogenesis of EXO involves invagination of late endosomes towards the lumen, forming multi-vesicular bodies (MVBs) wherein EXO are loaded with cargo [44,45]. The presence of TGFB1 and EXO in intraluminal vesicles of MVB for presumptive release was determined by immunogold-TEM in regDC (Figure 2A).

In addition to cytokines, EXO subtypes also contain miRNA and mRNA cargo that can influence functions of neighbouring cells [46]. Therefore, expression profiling of miRNAs in DC EXO subtypes was performed (Figure 2B) revealing prevalence in regDC EXO of downregulated inflammatory miRNAs (blue), while stimDC EXO have upregulated inflammatory miRNAs. Of particular note in regDC EXO, is 18-fold downregulation of proinflammatory miR155-5p [47] and 2-fold upregulation in stimDC EXO. Among mRNAs analysed, IL6 is worthy of mention as it was upregulated only in stimDC EXO (Figure 2C).
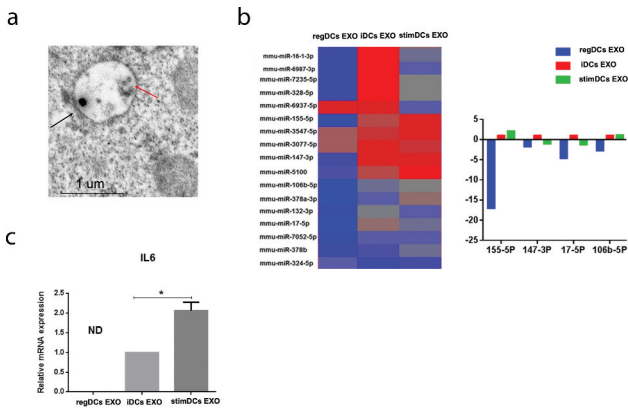

Figure 1. **RegDCs EXO protect encapsulated immunoregulatory cargo (TGFB1 and IL10) from proteolytic degradation**. (A) Nano-tracking analysis to determine EXO number and size distribution in nm. (B) Transmission electron microscopy (TEM) to visualize EXO shape and immuno-gold TEM to detect EXO marker tetraspanin CD63, showing unstained (left) and positive staining (right)(arrows). (C) Western blotting to detect other EXO-related markers including CD81, TSG101, GRP94 and B-actin in donor DCs and EXO (left) and anti/pro-inflammatory cytokines including TGFB1, IL10, IL6, IL1B and TNF and the costimulatory molecule CD86 as well as EXO associated proteins ALIX and TSG101 in DCs EXO subsets (right). (D) TGFB1 and IL10 content of lysed EXO and in regDCs EXO supernatant by ELISA. (E) TGFB1 and IL10 content of non-lysed EXO (transmembrane domain) by ELISA. (F) Immunogold TEM to detect luminal and transmembrane TGFB1 in regDCs EXO. (G) regDCs EXO (left) or equivalent concentration of free TGFB1 and IL10 (right) were treated with trypsin (upper panel) or proteinase-K (lower panel) and incubated in control buffer (1hour at 37°C) and analysed by western blotting to detect the levels of TGFB1, IL10 and exosomal markers TSG101 (upper panel) and CD81 (lower panel).
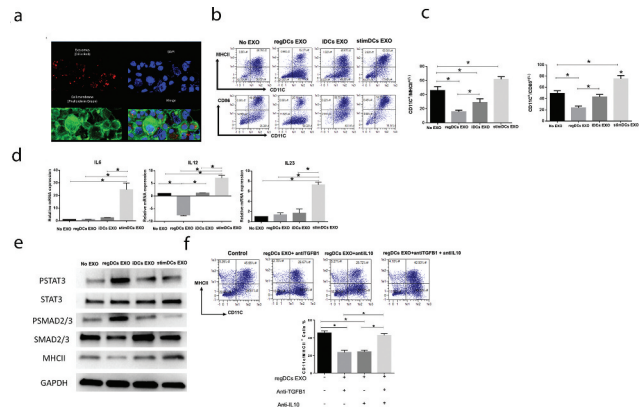
RegDC EXO induce an immune regulatory effect on acceptor DCs mediated by TGFB1 and IL10 in vitro

Co-culture of Dil-labelled regDC EXO with iDCs confirmed EXO internalization by acceptor DCs in vitro as shown by confocal microscopy analysis. Images show Dil-EXO (red) internalized by recipient DCs

Figure 2. **LPS/inflammation induced miRNAs and mRNA are down regulated in regDCs EXO in vitro**. (A) Colocalization of TGFB1 (back arrow) and EXO (red arrow) in multivesicular bodies in regDCs. (B) miRNA analysis of LPS/inflammation induced miRNAs in EXO. (C) IL6mRNA expression in EXO by PCR.

Figure 3. **DC EXO uptake by acceptor DCs, with EXO sub-type determining maturation and cytokine profile of acceptor DCs in vitro**. (A) Uptake of Dil labelled EXO (red) by bone marrow derived DCs, counterstained with nuclear stain DAPI (blue), phalloidin (green) for cell membrane and visualized under confocal microscopy. (B) Flow cytometry scattergrams showing % of (top panel) CD11c MHCII and (bottom panel) CD11c CD86 double positive cells in DCs treated or not treated with EXO (C) Bar graphs showing % of (left panel) CD11c MHCII and (right panel) CD11c CD86 double positive cells in DCs treated or not treated with each EXO subtype. (D) mRNA expression in DCs treated or not treated with EXO of IL6 (left panel), IL12 (middle panel) and IL23 (right panel). (E) Western blotting analysis of levels of phosphorylation of TGFB1and IL10 transcription factors, SMAD2/3 and STAT3 respectively and MHCII in DCs treated with or without EXO. (B) Flow cytometry scattergrams (top panels) showing % of double positive CD11c MHCII cells in DCs treated with or without regDCs EXO in presence or absence of neutralizing antibodies against TGFB1 and or IL10 and (bottom panel) representative bar graph. Results shown are representative of three independent experiments (* P<0.05 by one-way ANOVA followed by Tukeys multiple comparisons).

counterstained with phalloidin (green) (Figure 3A). Expression of co-stimulatory molecules required for T cell stimulation or maturation markers of acceptor iDCs were modulated by different EXO subtypes. This was evidenced by differential MHCII and CD86 expression on DCs shown by flow cytometry analysis. While reg DCs EXO significantly inhibited maturation markers of acceptor DCs, as evidenced by decrease in % CD11c$^+$ MHCII$^+$ and CD11c$^+$ CD86$^+$ expression, compared to control, stimDC EXO had the opposite effect, increasing %CD11c$^+$ MHCII$^+$ and CD11c$^+$ CD86$^+$expression, with iDC EXO-treated DCs intermediate of the two. (Figure 3B and Figure 3C). Cytokine profiling for IL-6, IL-12 and IL-23 mRNA further confirmed immuno-regulatory, – stimulatory or null phenotype of respective EXO (Figure 3D). iDCs co-cultured with DC EXO subtypes were analysed by immunoblot for activated transcription factors of IL-10 (pSTAT3) and TGFB1 (pSMAD2/3) signalling and total STAT3 and SMAD 2/3. RegDC EXO induced highest level of pSTAT3 and pSMAD2/3, consistent with TGFB-1 and IL-10-mediated signalling, respectively. RegDC EXO induced lowest level of MHCII (Figure 3E).

To assess the integrity and stability of EXO during incubation for multiple days in culture media, we performed immunoblot analysis of exosomal protein markers and loaded cytokines (TGFB and IL-10) in EXO after incubation in serum free culture media for 0, 1, 3, 5 and 7days. Results indicate that the EXO marker, Alix and the anti-inflammatory cytokine IL10, were stable until day 1 followed by a subtle decrease over time. However, stability of CD81 did not seem to be influenced by incubation for longer times. TGFB-1

showed stability at all time points (Fig. S2A). The size and zeta potential showed minimal changes (Fig S2B).

To determine the role of TGFB and IL-10 in inhibition of DC maturation by regDC EXO neutralizing antibodies to TGFB1 and IL10 were added. Complete restoration of MHCII expression was achieved by neutralization of both TGFB-1 and IL-10 while either one alone was not sufficient for restoration (Figure 3F). These results suggest the crucial role of both cytokines in the inhibition of acceptor DC maturation by regDC EXO.

RegDC EXO increase acceptor DC resistance to LPS mediated maturation and lower antigen presenting ability

RegDC EXO had the added capability to prevent *Escherichia coli* LPS-mediated maturation of iDCs, as evident by a significant decrease in MHCII (Figure 4A),

CD86 (Figure 4B) expression shown by flow cytometry analysis and downregulation of mRNA level of IL-6 (Figure 4C). The ability of DC EXO to regulate Ag-presentation in acceptor DCs was examined by proliferation of splenic OVA-specific T cells in response to OVA-iDCs. OVA-specific Ag-presentation by DCs was significantly reduced by regDC EXO and increased by stimDCs EXO-treated OVA-DCs (Figure 4D).

RegDC EXO is also taken up by CD4T-cells inhibiting proliferation and promoting TGFb1 mediated Tregs induction *in vitro*

Dil-labelled DC exo were co-cultured with splenic T cells to determine their ability to internalize DC exo. Scanning confocal microscopy revealed internalized regDC EXO inside Tcells (Figure 5A). Only regDC EXO significantly increased TCR-driven Tregs (CD25/FOXP3$^+$) induction, an effect that was abrogated by blocking TGFB-1 and not IL-10 using neutralizing antibody as shown by flow cytometry (Figure 5B and Figure 5C) and Western blotting (Figure 5D). These results suggest that TGFB-1 has a more dominant role in regulating Treg induction. RegDCs EXO also suppressed anti-CD3/CD28 antibodies mediated T cell proliferation while stimDC EXO increased proliferation in vitro (Figure 5E). StimDCs EXO were uniquely able to induce T-helper 17 cells, as measured by flow cytometry (Figure 5F) and ELISA (Figure 5G).
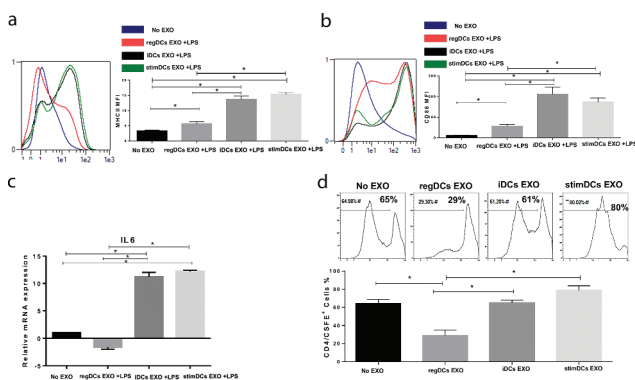
Figure 4. RegDCs EXO increase acceptor DC resistance to LPS mediated maturation and lower antigen presenting ability. Flow cytometry histograms showing in vitro influence of EXO subtypes on MHCII (A) and CD86 (B) expression on acceptor DCs challenged by LPS (left). Results presented as median fluorescent intensity measurements in representative bar graph (right). (C) IL-6 mRNA expression in acceptor DCs by PCR analysis. (D) Flow cytometry histograms showing proliferation of splenic ovalbumin specific CD4+T – cells, labelled with CFSE, after coculture with ovalbumin – pulsed DCs treated with or without EXO subtypes. Results shown are representative of three independent experiments (* P<0.05 by one-way ANOVA followed by Tukeys multiple comparisons).

To determine effects of T cells incubated with regDCs EXO on osteoclastogenesis, regDCs EXO-treated T cells were co-cultured with pre-osteoclasts, inhibiting osteoclastogenesis relative to non-EXO-treated control T cells, as demonstrated by TRAP staining (Fig. S3).

In vivo retention of DC EXO in gingival site of disease induction.

Initial *in vivo* studies focused on the bio distribution of EXO, 24hrs after IV or local palatal injection at the site of ligature-induced periodontitis (PD). Whole-body imaging in live mice of radiolabeled (In-111) DC EXO was performed using SPECT-CT. Control mice were administered equivalent activity of free In-111 by both routes. Free In-111 was rapidly cleared after IV administration, while In-111-labelled EXO were cleared slowly and bio distributed to spleen and other organs, but not maxilla (Figure 6A). In-111-labelled EXO administered in palatal maxillary tissue persisted at the site of experimental PD in maxilla, ostensibly from EXO adhesion to inflammatory integrins as reported [48], but also were observed in local lymph nodes. In contrast, free In-111 injected in the gingiva redistributed rapidly to other non-target extraoral body sites (Figure 6B). It should be noted that gingival injection of In-111-labelled EXO in inflamed diseased site yielded 10x higher radioactivity than injection of free In-111 (Figure 6C). Analysis of excised maxilla post-mortem also showed significant increase in radioactivity in In-111-labelled EXO injected group compared to free In-111, confirming *in vivo* SPECT-CT data (Figure 6D). Taken together, these data suggest higher retention of reg DC EXO in inflamed gingival tissue, where it persists exerting its action on resident immune cells leading to their reprogramming and modulation of immune response. 3D-video of In-111-labelled EXO biodistribution data are shown in Fig.S5.
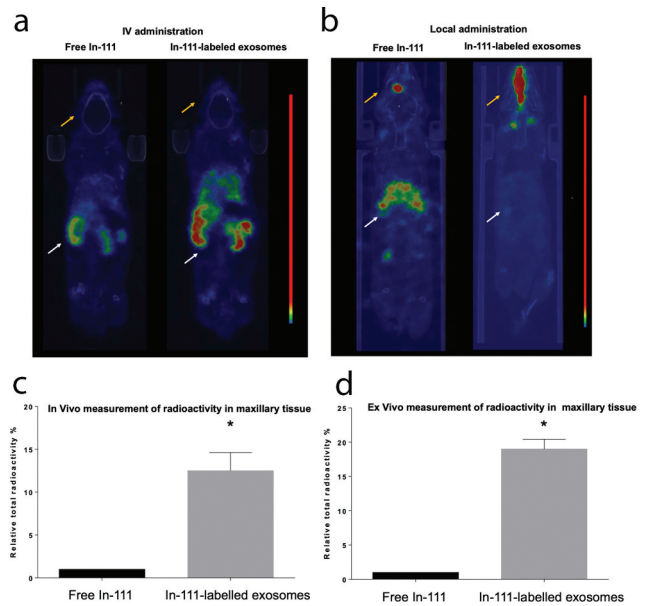
Uptake of injected EXO by gingival DCs/T cells, with subtypes differentially regulating DC maturation and Treg-Th17 infiltration in vivo

Mice were injected in the palatal gingiva with buffer (no EXO), Dil-labelled regDC EXO, iDC EXO, stimDC EXO, or TGFB/IL-10 (at equivalent concentrations to those carried in regDC EXO) in buffer on days −2, 0 and 2. Ligatures were placed on day 0 to promote bacterial accumulation and induce inflammatory alveolar bone loss, as detailed in materials and methods. Negative control group received neither ligatures nor EXO, while positive control group received ligatures but no EXO. On day 9, animals were sacrificed and disaggregated gingival cells were analysed by confocal microscopy for association of labelled EXO with
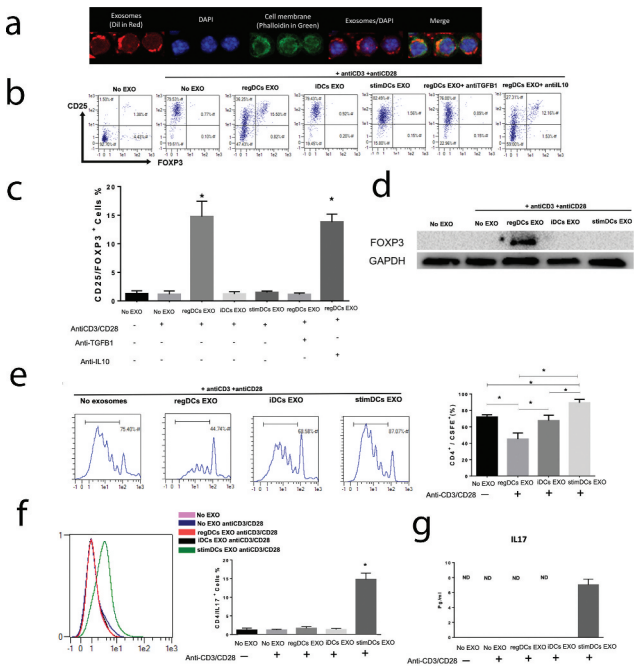
Figure 5. RegDCs EXO uptake by CD4T-cells, promoting TGFB1 dependent Tregs induction while stim DCs EXO induce T-helper17 response in vitro. (A) Uptake of Dil labelled EXO (red) by splenic CD4T-cells, showing DAPI-labelled nuclei, and phalloidin (green) labelled cell membrane, as visualized under confocal microscopy. (B) Flowcytometry scattergrams showing in vitro influence of EXO on induction of T-regulatory cells, as measured by % of double positive CD25 and Foxp3 cells in gated CD4T-cell population, stimulated with antiCD3/CD28 antibodies. (C) Summary bar graph of flow cytometry data. (D) Western blotting analysis of Foxp3 expression in acceptor CD4T-cells. (E) Flow cytometry analysis showing proliferation % of CFSE-labelled splenic CD4+T-cells, as expressed by histograms (left panel) and bar graphs (right panel), after stimulation with anti-CD3/CD28 in presence or absence of EXO subtypes. (F) Flow cytometry analysis of CD4+IL-17+T cells %, as expressed by histograms (left) and bar graph (right). (G) ELISA of IL17 expression in supernatant of T cells treated with EXO subtypes. Results shown are representative of three independent experiments (* P<0.05 by one-way ANOVA followed by Tukeys multiple comparisons).


Figure 6. Locally administrated exosomes showed higher affinity and slower clearance from periodontal tissues in inflammatory alveolar bone loss model. (A) SPECT CT live animal in vivo imaging of free In-111 (left) or In-111-labelled exosomes (right) in mice after 24h of IV administration. (B) Local delivery of free In-111 (left) or In-111-labelled exosomes (right) by injection in the palatal gingiva at the right side of maxilla was utilized. (C) Radioactivity in maxilla, relative to total, when free or bound to DC EXO, expressed as % determined using SPECT CT images. (D) Radioactivity in maxilla, relative to total, when free or bound to DC EXO, expressed as %, in post-mortem isolated maxilla, determined by gamma counter. Mice were subjected to ligature placement to induce inflammatory bone loss prior to imaging. Yellow arrows delineate maxilla, white arrows liver, spleen and other non-oral sites.

CD11c+DCs and CD4+T cells. Both DCs (Figure 7A) and T-cells (Figure 8A) are observed colocalized with EXO *in situ*. The influence of EXO on gingival DC maturation status was determined by flow cytometry analysis of MHCII and CD86 expression on isolated CD11c+DCs from 6 experimental groups. As observed in vitro, regDC EXO injected in vivo induced significant decrease in MHCII and CD86 expression (Figure 7(B, C)) on gingival DCs, further confirmed by immunohistochemical staining for CD86 (Figure 7D and Figure 7E). Furthermore, only in the regDC EXO-treated group was a significant increase in Tregs and decrease in %CD4+IL-17+T cells observed (Figure 8(B, C)). Analysis of FOXP3, CTLA4 and IL10 mRNA

further confirms the immunoregulatory influence of regDs EXO *in situ* (Figure 8C). Immunohistochemical analysis of gingival tissue *in situ* revealed higher positive staining for Foxp3 (Figure 8D) and lower positive staining for IL17 (Figure 8E) in regDC EXO + ligature-treated group in comparison to no EXO +ligature group. Due to observed bio distribution of labelled EXO to local lymph nodes, CD4+T cells were quantified in draining lymph nodes, revealing a significant decrease in frequency of CD4T-cells in regDC EXO-treated group (Fig. S4A and Fig. S4B). These data show that both in vitro and in vivo, regDCS EXO-mediated reprogramming of DCs and T cells towards an immune modulatory phenotype.

Differential regulation of local bone resorbing mediators and osteoclastic density by DC EXO subtypes

Analysis of mRNA in gingival tissues from experimental groups reveals a significant decrease in RANKL (Figure 9A) and TNF (Figure 9B) in regDC EXO-injected group
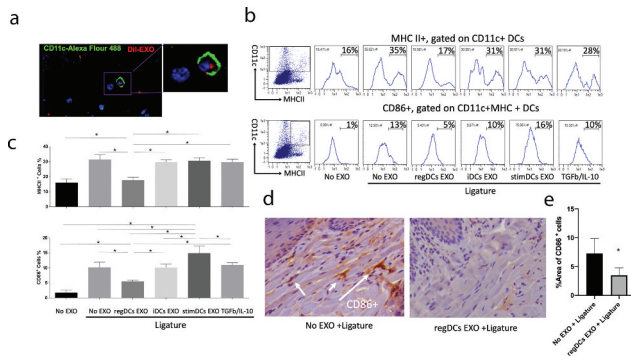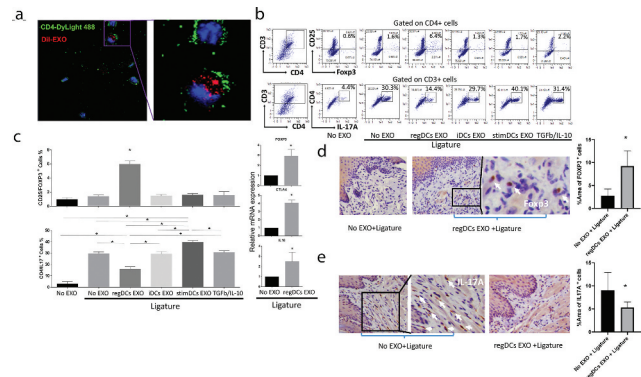
Figure 7. RegDCs EXO co-localize with gingival acceptor DCs, inhibiting maturation in alveolar bone loss model. DIL (Red) labelled EXO were injected into the palatal gingiva of the upper right second molar of inflammatory alveolar bone loss model at days −2, 0 and 2 relatives to ligature placement. At day 9 gingival tissues were harvested and dissected for cell isolation. Immunofluorescence labelling of cells was performed using Alexa Flour 488-labelled anti CD11c to identify dendritic cells, counterstained with nuclear stain DAPI and visualized under confocal microscopy. (A) Co-localization of EXO (red) with nucleus (DAPI) and dendritic cells (green). (B) Flow cytometry analysis of MHCII+ cells % in CD11c+DCs gate (top histograms) and CD86+cells % in MHCII+ CD11c+DCs gate (bottom histograms) in gingival cells isolated from six tested groups. (C) Bar graphs of flow cytometry data from (B) showing statistically significant differences in the groups. (D) Representative immunohistochemical staining of CD86+presumptive DCs (arrows) in lamina propria of gingival tissue sections of (left) no EXO-treated +ligature and (right) regDCs EXO-treated +ligature groups. (E) Bar graph of immunohistochemical staining data from (D) showing statistically significant differences in the groups. N=5 in each group; * P<0.05 by one-way ANOVA, followed by Tukeys multiple comparisons.

Figure 8. RegDCs EXO interact with gingival CD4T-cells, inducing Tregs and inhibiting Th17 recruitment in vivo. DIL (red) labelled EXO were injected into palatal gingiva of the upper right second molar at days −2, 0 and 2 relatives to ligature placement. At day 9 gingival tissue were harvested and dissected for cell isolation. Immunofluorescence labelling of cells were performed with Dylight 488 labelled-anti-CD4 (green) to identify CD4-T cells and DAPI for nucleus and visualized under confocal microscopy. (A) Co-localization of EXO with nucleus (DAPI) and CD4T-cell (green). (B) Scattergrams from flow cytometry analysis of CD25+Foxp3+Tregs % (top panels) and CD4+IL-17A+ Th17 cells % (bottom panels), gated on CD4+and CD3+lymphocytes, respectively, in the gingival cells isolated from the six tested groups. (C) (Left) Bar graphs of CD25+Foxp3+Tregs % (upper panel) and CD4+IL-17A + Th17 cells % (lower panel) in all groups from (B), and (Right) mRNA levels of (top) Foxp3, (middle) CTLA4 and (bottom) IL-10 in: no EXO vs regDCs EXO-treated groups + ligature. Representative immunohistochemical staining and bar graphs of (D) Foxp3 and (E) IL-17A in lamina propria of gingival tissue sections of (left) no EXO-treated +ligature group and (right) regDCs EXO-treated +ligature group. White arrows delineate positive staining. N=5 in each group; * P<0.05 by one-way ANOVA, followed by Tukeys multiple comparisons.

relative to other ligature-treated groups, including free TGFB/IL-10 group. Immunohistochemical analysis of gingival tissue revealed lower positive staining for RANKL (Figure 9C) and TNF (Figure 9D) in regDC EXO + ligature-treated group in comparison to no EXO + ligature group. TRAP staining of bone sections revealed significant decrease in osteoclastic density in regDC EXO-treated + ligature group, in comparison to other ligature-treated groups, while stimDCs EXO group showed particularly high TRAP staining (Figure 9E and F). These results provided evidence from cellular immune and histologic standpoints, with putative mechanisms involved, that regDCs EXO would effectively inhibit inflammatory alveolar bone loss.

Regulation of ligature-induced alveolar bone loss by DC EXO subtypes

De-fleshed maxillae from EXO-treated and untreated mice were analysed for bone loss, volumetrically, using microCT. 3-D images of bone volume are shown (Figure 10A). Quantitative analysis confirms 35%

bone loss induced by ligature-induced inflammation in the absence of EXO. Injection of regDC EXO reduced alveolar bone loss significantly (p<0.05), while stimDC EXO increased bone loss, with control immune null iDCs EXO and free TGFb/IL-10 intermediate of the two (Figure 10B). The lack of efficacy of free TGFb/IL-10 emphasizes the importance of EXO encapsulation of cargo to protect it from proteolytic degradation (Figure 1G) and promote its persistence at diseased site (Figure 6). Histological sections confirm bone changes observed in volumetric microCT data (Figure 10C). These results further substantiate the hypothesis that regDCs EXO, loaded with TGFb and IL-10 reprogram the immune response and inhibit inflammatory bone loss.
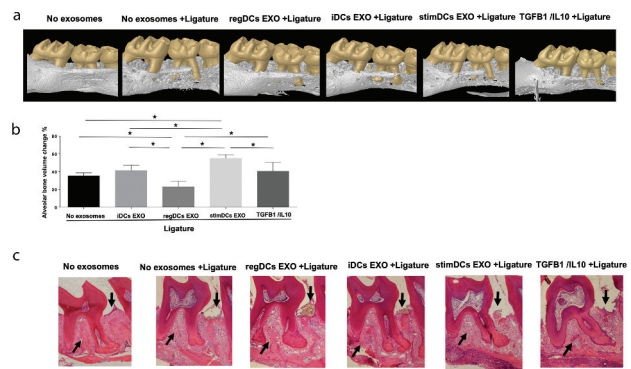
Discussion

The role of Tregs in dampening inflammatory Th17 responses, inhibiting autoimmune disorders, graft
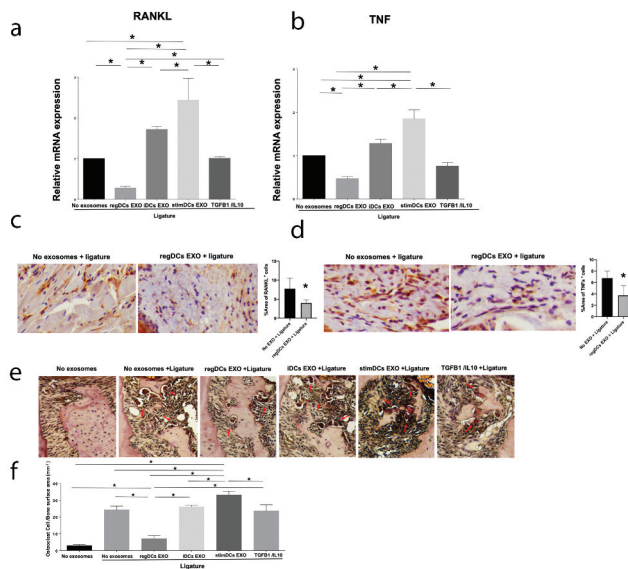
Figure 9. **RegDCs EXO inhibit RANK-L, TNFa and TRAP+ osteoclast induction**. mRNA expression of RANKL (A) and TNFa (B) in gingival tissue of ligature groups that received indicated EXO subtypes or no EXO. Representative immunohistochemical stained sections and bar graphs showing expression of (C) RANKL and (D) TNFa in lamina propria of gingival tissue sections treated with no EXO + ligature or regDCs EXO + ligature. (E) Representative Trap+staining of periodontal tissue sections in EXO subtypes + ligature or no EXO and no ligature or ligature alone treated groups. (F) Bar graph showing quantification of Trap positive multinucleated cell per bone surface area in interdental area, three slides per animal. N=5 in each group; * P<0.05 by one-way ANOVA followed by Tukeys multiple comparisons.

Figure 10. **RegDCs EXO inhibit, stimDC EXO promote inflammatory bone loss**. (A) Representative microCT generated 3-D images of upper right maxilla with teeth. (B) Bar graphs of alveolar bone volume change % based on quantification of the whole 3-D alveolar bone volume around upper second molar (ligature placement site) by micro CT and normalization to the measurement obtained from the contralateral side (no ligature) which served as baseline, followed by normalization to the alveolar bone volume around the upper right second molar of group that did not receive ligature or exosomes (N=5 in each group; * P<0.05 by one-way ANOVA followed by Tukeys multiple-comparisons). (C) Histological sections showing distinct levels of alveolar bone in furcation area and interdental bone (arrows) of upper right second molar of tested groups.

rejection and alveolar bone loss is previously reported [21,23,49–55]. However, there are no published reports of DC-derived EXO being used to reprogram the Th17 mediated immune response to attenuate alveolar bone loss. EXO are naturally released from cells, and endowed with surface adhesion proteins that promote higher interaction and cellular uptake capacity, in comparison to other synthetic agents like liposomes and other nanoparticles which may be toxic [27,29,56,57]. Clinical trials have shown the feasibility and safety of DC-derived EVs administration in melanoma [58], non-small lung cancer [59] and advanced non-small lung cancer [60]. Other therapeutic applications include colon cancer [61] cutaneous ulcers, and mesenchymal stem cell derived EXO for type I diabetes mellitus [26]. Despite excitement of EXO therapy for a variety of human diseases, no published study to our knowledge has examined DC EXO as an immunotherapeutic agent for inflammatory alveolar bone loss. Our data suggest that TGFB1- and IL10-loaded DC EXO shield cytokines from proteolytic attack, are retained in periodontal tissues and taken

up by DCs and T-cells in gingiva, modulating their phenotype and functions *in vivo*, resulting in inhibition of alveolar bone loss.

TGFB1 is an immunoregulatory cytokine with differential effects on immune cells, including direct inhibition of effector T-cell activation and proliferation, inhibition of maturation of DCs and macrophages and induction of T-regulatory cells [62,63]. IL-10 is also an immunoregulatory cytokine that inhibits immune cell activation and pro-inflammatory cytokine release that contribute to inflammatory bone loss such as TNF, IL6 and IL17 and RANKL [21]. Moreover, TGFB1 and IL-10 have synergistic regulatory effects [64,65]. Using antibody inhibition studies, we have shown the crucial role of TGFB-1 and IL-10 in the induction of regulatory immune response by regDCs EXO *in vitro*, with TGFB1 the dominant driving force for Treg differentiation (Figure 5(B, C)) while both cytokines are required for inhibition of DC maturation (Figure 3F). However, the exact mechanism of TGFB-1 interaction with target cells remains to be fully understood.

Our data has shown that TGFB-1 is localized on the outer surface of the EXO as well as inside the EXO as shown by TEM and ELISA (Figure 1(D, E, F). The EXO-associated TGFB-1 was protected from degradation by trypsin and partially protected from proteinase-

K. (Figure 1G). This may be due to the protective effect of double membrane on EXO for cytokines in its lumen, as well as three-dimensional structure of cytokines [66] embedded in the transmembrane domain.

The interactions between reg DC EXO and acceptor cells are under intensive investigation in our laboratory. Two principal mechanisms, not mutually exclusive, are proposed, involving EXO binding to cell surface receptors, stimulating downstream signalling of SMAD2 phosphorylation, as well as EXO internalization by target cell where it unloads its cargo. A third mechanism could be through the slow release of TGFB-1 from the EXO to the extracellular matrix promoting a paracrine effect on the recipient cell [66–69]. A recent study has shown that neutralizing TGFB-1 on the surface of EXO as well as blocking of TGFBR-1 inhibited SMAD2 signalling [66], alluding to the importance of surface TGFB-1 in the function of EXO . This suggests that an initial interaction of EXO-associated TGFB with TGF-B1 receptor complex is paramount. The same study showed that the EXO facilitates the internalization of EXO-TGFB-1 receptor complex. Within the recipient cell, trafficking of the exosome occurs through endosomal translocation, rather than lysosomal degradation [66,69,70]. A recent study has localized EXO-associated TGFB1 bound to its receptor within endosomal compartments [66] and not in lysosomal compartments, suggesting that EXO protect TGFB-1 from lysosomal degradation. The acidic endosomal compartments would then lead to the release of TGFB-1 bound to its receptor resulting in prolonged sustained SMAD2 signalling [66].

Another suggested mechanism is that after EXO internalization into the recipient cell, TGFB-1 released inside the cell is recycled and shuttled back to the cell membrane where it is secreted to act on the cell surface receptor in an autocrine manner [68]. These results collectively suggest that the mechanism of action of TGFB-1 bearing EXO on the recipient cells requires an initial interaction with the cell surface receptor. However, the internalization of EXO and its endosomal translocation are essential for a sustainable prolonged signalling. Further studies are required to unravel the exact mechanism of communication between EXO and recipient cell.

Unencapsulated TGFB1 and IL-10, injected into gingiva in buffer, did not induce Treg recruitment (Figure 8(B, C)) or inhibit inflammatory bone loss (Figure 10(A, B, C)). Free TGFB1 and IL-10 are likely cleared and degraded rapidly in *vivo* at the disease site. DC EXO prevent proteolytic degradation of EXO encapsulated cytokines (Figure 1G). Moreover, DC EXO persist at the disease site (Figure 6). DC EXO express a variety of adhesion molecules, tetraspanins, integrins and lectins that could promote inflammatory cell binding persistence at the inflamed site [70]. In the present study, three injections of regDC EXO were sufficient to inhibit *in situ* DC maturation (Figure 7), increasing Tregs and decreasing Th17 effectors locally (Figure 8) and attenuate inflammatory bone loss (Figure 10). Evidence further documents the physical uptake of DC EXO by DCs and T-cells *in vitro* (Figure 3A and Figure 5A) and *in vivo* in gingival tissues (Figure 7A and Figure 8A). The mechanisms of EXO uptake by recipient DCs and T cells are critical determinants of the ensuing cellular response [45], and are thus being studied by our group outside the purviews of this work.

In a previous elegant approach to attenuate bone loss, CCL22-loaded synthetic micro-particles were injected to recruit gingival Tregs [21]. Distinct differences in our study included the use of DC-derived nanoparticles [45] to deliver either anti-, or pro-inflammatory cytokine cargo to the site of disease, and assess its potential for predictable disease resolution or exacerbation. Moreover, alveolar bone loss volume in 3-D, was measured by microCT. Our study further traced the anatomical fate of DC EXO in whole live animals, revealing EXO distribution to spleen and other organs when injected by IV route, versus its persistence in the gingiva upon local administration (Figure 6). Our findings are consistent with promising reports of DC EXO therapy for other inflammatory disease models, such as colitis and encephalitis, although adenovirus transfected DC EXO, that secrete TGFB1 were used. While mitigation of Th17 responses were commensurate with clinical improvement [71,72], use of adenovirus raises immunogenicity, toxicity and transformation concerns. The present study used recombinant TGFB1 and IL10, isolated from non-genetically modified DCs to passively and actively load EXO. StimDC EXO were not actively loaded with pro-inflammatory cytokines, but nonetheless enhanced Th17 induction and inflammatory bone loss. The role of Th17 effectors in bone degeneration is well established [13,22,73,74]. Here we show the mechanism involves downregulation of bone resorbing cytokines RANKL and TNF and reduction of TRAP+ osteoclasts *in vivo* (Figure 9).We also showed that regDC EXO-treated T-cells could inhibit osteoclastogenesis *in vitro* (Fig. S3), suggesting their bone protective effect [75,76].

DC EXO contain other cargo including mRNA, miRNA and additional proteins that could influence recipient cell functions *in vitro* and *in vivo*. We therefore examined distinct miRNA profiles in DC EXO subtypes (Figure 2B). Worthy of emphasis is miR155-5p, downregulated in regDC EXO, upregulated in stimDC EXO. Reported functions of miR155-5p in recipient immune cells include increased induction of pro-inflammatory mediators and decrease in programmed death ligand-1 (PD-L1) [47].

EXO-bound miRNAs are recognized as novel endogenous targets for therapeutic treatments [77]. Determining functions of specific miRNA cargo in these DC EXO, including generation of mimics/anti-mimics is in planning stages.

The DC EXO subtypes used here contain a constellation of other surface bound and encapsulated proteins coding and non-coding RNA that need to be definitively characterized so that we can better understand the immunobiology of DC EXO. Efforts in our laboratory are focused on LC/MS/MS characterization of DC EXO proteins, identifying shared and unique pathways, biological processes and metabolic functions.

In summary, the feasibility and efficacy of DCs EXO loaded with anti-inflammatory cargo as a therapeutic approach to experimental degenerative bone disease was established. The immunologic mechanisms responsible for inhibition (or acceleration) of bone loss in this model was further delineated by using immuno-stimulatory and immune null DC EXO. A more targeted engineering approach, with defined surface proteins and molecular cargo into null DC EXO is in progress.

Funding

ORCID

Mahmoud Elashiry ⓘD http://orcid.org/0000-0001-7077-2725
Christopher W. Cutler ⓘD http://orcid.org/0000-0003-4396-4072

References

[1] Eke PI, Dye BA, Wei L, et al. Update on prevalence of Periodontitis in Adults in the USA: NHANES 2009 to 2012. J Periodontol. 2015;86:611–622. published online EpubMay.

[2] Carrion J, Scisci E, Miles B, et al., Microbial carriage state of peripheral blood dendritic cells (DCs) in chronic periodontitis influences DC differentiation, atherogenic potential. J Immunol 189, 3178–3187; published online Epub Sep 15 (). 2012

[3] Teixeira FB, Saito MT, Matheus FC, et al. Periodontitis and Alzheimer's disease: a possible comorbidity between oral chronic inflammatory condition and neuroinflammation. Front Aging Neurosci. 2017;9:327.

[4] Bartold PM, Van Dyke TE. An appraisal of the role of specific bacteria in the initial pathogenesis of periodontitis. J Clin Periodontol. 2019 Jan;46:6–11. published online Epub.

[5] Jotwani R, Cutler CW. Multiple dendritic cell (DC) subpopulations in human gingiva and association of mature DCs with CD4+ T-cells in situ. J Dent Res. 2003 Sep;82:736–741. published online Epub. .

[6] Jotwani R, Muthukuru M, Cutler CW. Increase in HIV receptors/co-receptors/alpha-defensins in inflamed human gingiva. J Dent Res. 2004 May;83:371–377. published online Epub. .

[7] Jotwani R, Palucka AK, Al-Quotub M, et al. Mature dendritic cells infiltrate the T cell-rich region of oral mucosa in chronic periodontitis: in situ, in vivo, and in vitro studies. J Immunol. 2001 Oct 15 published online Epub;167: 4693–4700.

[8] Arjunan P, Meghil MM, Pi W, et al. Oral Pathobiont activates anti-apoptotic pathway, promoting both immune suppression and oncogenic cell proliferation. Sci Rep. 2018 Nov 9;8:16607.

[9] Barone F, Bombardieri M, Manzo A, et al. Association of CXCL13 and CCL21 expression with the progressive organization of lymphoid-like structures in Sjogren's syndrome. Arthritis Rheum. 2005 Jun;52:1773–1784. published online Epub.

[10] Bergomas F, Grizzi F, Doni A, et al. Tertiary intratumor lymphoid tissue in colo-rectal cancer. Cancers (Basel). 2011 Dec 28;4:1–10.

[11] Dudek AM, Martin S, Garg AD, et al. Immature, semi-mature, and fully mature dendritic cells: toward a dc-cancer cells interface that augments anticancer immunity. Front Immunol. 2013;4:438.

[12] Park SJ, Nakagawa T, Kitamura H, et al. IL-6 regulates in vivo dendritic cell differentiation through STAT3 activation. J Immunol. 2004 Sep 15 published online Epub;173: 3844–3854.

[13] Tsukasaki M, Komatsu N, Nagashima K, et al. Host defense against oral microbiota by bone-damaging T cells. Nat Commun. 2018 Feb 16;9:701.

[14] Horton C, Shanmugarajah K, Fairchild PJ. Harnessing the properties of dendritic cells in the pursuit of immunological tolerance. Biomed J. 2017 Apr;40:80–93. published online Epub.

[15] Jonuleit H, Schmitt E, Schuler G, et al. Induction of interleukin 10-producing, nonproliferating CD4(+) T cells with regulatory properties by repetitive stimulation with allogeneic immature human dendritic cells. J Exp Med. 2000 Nov 6;192:1213–1222.

[16] Idoyaga J, Fiorese C, Zbytnuik L, et al. Specialized role of migratory dendritic cells in peripheral tolerance induction. J Clin Invest. 2013 Feb;123:844–854. published online Epub.

[17] Hasegawa H, Matsumoto T. Mechanisms of tolerance induction by Dendritic cells in vivo. Front Immunol. 2018;9:350.

[18] Komatsu N, Takayanagi H. Immune-bone interplay in the structural damage in rheumatoid arthritis. Clin Exp Immunol. 2018;194:1–8.

[19] Dutzan N, Kajikawa T, Abusleme L, et al. A dysbiotic microbiome triggers TH17 cells to mediate oral mucosal immunopathology in mice and humans. Sci Transl Med. 2018 Oct 17;10:eaat0797.

[20] Garlet GP, Cardoso CR, Mariano FS, et al. Regulatory T cells attenuate experimental periodontitis progression in mice. J Clin Periodontol. 2010 Jul;37:591–600. published online Epub.

[21] Glowacki AJ, Yoshizawa S, Jhunjhunwala S, et al. Prevention of inflammation-mediated bone loss in murine and canine periodontal disease via recruitment of regulatory lymphocytes. Proc Natl Acad Sci U S A. 2013 Nov 12;110:18525–18530.

[22] Rajendran M, Looney S, Singh N, et al. Systemic antibiotic therapy reduces circulating inflammatory Dendritic cells and Treg-Th17 plasticity in Periodontitis. J Immunol. 2019 May 1;202:2690–2699.

[23] Ezzelarab M, Thomson AW. Tolerogenic dendritic cells and their role in transplantation. Semin Immunol. 2011 Aug;23:252–263. published online Epub.

[24] Kim SH, Lechman ER, Bianco N, et al. Exosomes derived from IL-10-treated dendritic cells can suppress inflammation and collagen-induced arthritis. J Immunol (Baltimore, Md: 1950). 2005 May 15;174:6440–6448.

[25] Clayton A, Harris CL, Court J, et al. Antigen-presenting cell exosomes are protected from complement-mediated lysis by expression of CD55 and CD59. Eur J Immunol. 2003 Feb;33:522–531. published online Epub.

[26] Mentkowski KI, Snitzer JD, Rusnak S, et al. Therapeutic potential of engineered extracellular vesicles. Aaps J. 2018 Mar 15;20:50.

[27] Haney MJ, Klyachko NL, Zhao Y, et al. Exosomes as drug delivery vehicles for Parkinson's disease therapy. J Control Release. 2015 Jun 10;207:18–30.

[28] Qazi KR, Gehrmann U, Domange Jordo E, et al. Antigen-loaded exosomes alone induce Th1-type memory through a B-cell-dependent mechanism. Blood. 2009 Mar 19;113:2673–2683.

[29] Kim MS, Haney MJ, Zhao Y, et al. Development of exosome-encapsulated paclitaxel to overcome MDR in cancer cells. Nanomed. 2016 Apr;12:655–664. published online Epub.

[30] Segura E, Valladeau-Guilemond J, Donnadieu MH, et al. Characterization of resident and migratory dendritic cells in human lymph nodes. J Exp Med. 2012 Apr 9;209:653–660.

[31] Yin W, Ouyang S, Li Y, et al. Immature dendritic cell-derived exosomes: a promise subcellular vaccine for autoimmunity. Inflammation. 2013 Feb;36:232–240. published online Epub.

[32] Muccioli M, Pate M, Omosebi O, et al. Generation and labeling of murine bone marrow-derived dendritic cells with Qdot nanocrystals for tracking studies. J Vis Exp. 2011 Jun 2. published online Epub. DOI:10.3791/2785

[33] Helwa I, Cai J, Drewry MD, et al. A comparative study of serum exosome isolation using differential ultracentrifugation and three commercial reagents. PLOS One. 2017;12: e0170628.

[34] Mehdiani A, Maier A, Pinto A, et al. An innovative method for exosome quantification and size measurement. J Vis Exp. 2015 Jan 17:50974 published online Epub. DOI:10.3791/50974.

[35] Dinkins MB, Enasko J. Neutral Sphingomyelinase-2 deficiency Ameliorates Alzheimer's Disease pathology and improves cognition in the 5XFAD Mouse. J Neurosci. 2016 Aug 17;36:8653–8667. published online Epub.

[36] Wang Y, Zhang L, Li Y, et al. Exosomes/microvesicles from induced pluripotent stem cells deliver cardioprotective miRNAs and prevent cardiomyocyte apoptosis in the ischemic myocardium. Int J Cardiol. 2015 Aug 1;192:61–69.

[37] Nirvani M, Khuu C, Utheim TP, et al. Circadian rhythms and gene expression during mouse molar tooth development. Acta Odontol Scand. 2017 Mar;75:144–153. published online Epub.

[38] Eskan MA, Jotwani R, Abe T, et al. The leukocyte integrin antagonist Del-1 inhibits IL-17-mediated inflammatory bone loss. Nat Immunol. 2012 Mar 25;13:465–473.

[39] Qin X, Hoda MN, Susin C, et al. Increased innate lymphoid cells in periodontal tissue of the murine model of Periodontitis: the role of AMP-activated protein Kinase and relevance for the human condition. Front Immunol. 2017;8:922.

[40] Rashid MH, Borin TF, Ara R, et al. Differential in vivo biodistribution of (131)I-labeled exosomes from diverse cellular origins and its implication for theranostic application. Nanomed. 2019 Aug 1;21:102072.

[41] Elsayed R, Abraham P, Awad ME, et al. Removal of matrix-bound zoledronate prevents post-extraction osteonecrosis of the jaw by rescuing osteoclast function. Bone. 2018 May;110:141–149. published online Epub.

[42] Lee CT, Teles R, Kantarci A. Resolvin E1 reverses experimental Periodontitis and Dysbiosis. J Immunol. 2016 Oct 1;197:2796–2806. published online Epub.

[43] Li X, Li X, Lin J, et al. Exosomes derived from low-intensity pulsed ultrasound-treated Dendritic cells suppress tumor necrosis factor-induced Endothelial inflammation. J Ultrasound Med. 2018 Dec 18. published online Epub. DOI:10.1002/jum.14898

[44] Colombo M, Raposo G, Thery C. Biogenesis, secretion, and intercellular interactions of exosomes and other extracellular vesicles. Annu Rev Cell Dev Biol. 2014;30:255–289.

[45] McKelvey KJ, Powell KL, Ashton AW, et al. Exosomes: mechanisms of Uptake. J Circ Biomark. 2015;4:7.

[46] Nazarenko I, Rupp AK, Altevogt P. Exosomes as a potential tool for a specific delivery of functional molecules. Methods Mol Biol. 2013;1049:495–511.

[47] Yee D, Shah KM, Coles MC, et al. MicroRNA-155 induction via TNF-alpha and IFN-gamma suppresses expression of programmed death ligand-1 (PD-L1) in human primary cells. J Biol Chem. 2017 Dec 15;292:20683–20693.

[48] Morelli AE, Larregina AT, Shufesky WJ, et al. Endocytosis, intracellular sorting, and processing of exosomes by dendritic cells. Blood. 2004 Nov 15;104:3257–3266.

[49] Cools N, Van Tendeloo VF, Smits EL, et al. Immunosuppression induced by immature dendritic cells is mediated by TGF-beta/IL-10 double-positive CD4+ regulatory T cells. J Cell Mol Med. 2008 Apr;12:690–700. published online Epub.

[50] Oh K, Kim YS, Lee DS. Maturation-resistant dendritic cells ameliorate experimental autoimmune uveoretinitis. Immune Netw. 2011 Dec;11:399–405. published online Epub.

[51] Sun X, Gong ZJ, Wang ZW, et al. IDO-competent-DCs induced by IFN-gamma attenuate acute rejection in rat liver transplantation. J Clin Immunol. 2012 Aug;32:837–847. published online Epub.

[52] Arizon M, Nudel I, Segev H, et al. Langerhans cells down-regulate inflammation-driven alveolar bone loss. Proc Nat Acad Sci. 2012;109:7043–7048.

[53] Riley JL, June CH, Blazar BR. Human T regulatory cell therapy: take a billion or so and call me in the morning. Immunity. 2009;30:656–665.

[54] Trzonkowski P, Bacchetta R, Battaglia M, et al. Hurdles in therapy with regulatory T cells. Sci Transl Med. 2015;7:304ps318–304ps318.

[55] Alissafi T, Banos A, Boon L, et al. Tregs restrain dendritic cell autophagy to ameliorate autoimmunity. J Clin Invest. 2017 Jun 30;127:2789–2804.

[56] Zhuang X, Xiang X, Grizzle W, et al. Treatment of brain inflammatory diseases by delivering exosome encapsulated anti-inflammatory drugs from the nasal region to the brain. Mol Ther. 2011;19:1769–1779.

[57] Sun D, Zhuang X, Xiang X, et al. A novel nanoparticle drug delivery system: the anti-inflammatory activity of curcumin is enhanced when encapsulated in exosomes. Mol Ther. 2010;18:1606–1614.

[58] Escudier B, Dorval T, Chaput N, et al. Vaccination of metastatic melanoma patients with autologous dendritic cell (DC) derived-exosomes: results of the first phase I clinical trial. J Transl Med. 2005 Mar 2;3:10.

[59] Morse MA, Garst J, Osada T, et al. A phase I study of dexosome immunotherapy in patients with advanced non-small cell lung cancer. J Transl Med. 2005 Feb 21;3:9.

[60] C. M, Besse B, Lapierre V, et al. Dendritic cell-derived exosomes as maintenance immunotherapy after first line chemotherapy in NSCLC. Oncoimmunology. 2016;5:e1071008.

[61] W. D, Dai S, Wu Z, et al. Phase I clinical trial of autologous ascites-derived exosomes combined with GM-CSF for colorectal cancer. Mol Ther. 2008;16:782–790.

[62] Tran DQ. TGF-β: the sword, the wand, and the shield of FOXP3+ regulatory T cells. J Mol Cell Biol. 2011;4:29–37.

[63] Ihara S, Hirata Y, Koike K. TGF-β in inflammatory bowel disease: a key regulator of immune cells, epithelium, and the intestinal microbiota. J Gastroenterol. 2017;52:777–787.

[64] Guo B. IL-10 modulates Th17 pathogenicity during autoimmune diseases. J Clin Cell Immunol. 2016;7. doi:10.4172/2155-9899.1000400

[65] Iyer SS, Cheng G. Role of interleukin 10 transcriptional regulation in inflammation and autoimmune disease. Crit Rev™ Immunol. 2012;32: 23–63.

[66] Shelke GV, Yin Y, Jang SC, et al. Endosomal signalling via exosome surface TGFbeta-1. J Extracell Vesicles. 2019;8:1650458.

[67] Jakhar R, Crasta K. Exosomes as emerging pro-tumorigenic mediators of the senescence-associated secretory phenotype. Int. J. Mol. Sci. 2019 May 24;20:2547.

[68] Ringuette Goulet C, Bernard G, Tremblay S, et al. Exosomes induce fibroblast differentiation into cancer-associated fibroblasts through TGFbeta signaling. Mol Cancer Res. 2018 Jul;16:1196–1204. published online Epub.

[69] van Dongen HM, Masoumi N, Witwer KW, et al. Extracellular vesicles exploit viral entry routes for cargo delivery. Microbiol Mol Biol Rev. 2016 Jun;80:369–386. published online Epub.

[70] Mulcahy LA, Pink RC, Carter DR. Routes and mechanisms of extracellular vesicle uptake. J Extracell Vesicles. 2014;3:24641.

[71] Cai Z, Zhang W, Yang F, et al. Immunosuppressive exosomes from TGF-β1 gene-modified dendritic cells attenuate Th17-mediated inflammatory autoimmune disease by inducing regulatory T cells. Cell Res. 2012;22:607.

[72] Yu L, Yang F, Jiang L, et al. Exosomes with membrane-associated TGF-β1 from gene-modified dendritic cells inhibit murine EAE independently of MHC restriction. Eur J Immunol. 2013;43:2461–2472.

[73] Eskan MA, Jotwani R, Abe T, et al. The leukocyte integrin antagonist Del-1 inhibits IL-17-mediated inflammatory bone loss. Nat Immunol. 2012;13:465.

[74] Moutsopoulos NM, Konkel J, Sarmadi M, et al. Defective neutrophil recruitment in leukocyte adhesion deficiency type I disease causes local IL-17–driven inflammatory bone loss. Sci Transl Med. 2014; 6:229ra240–229ra240.

[75] Kim YG, Lee CK, Nah SS, et al. Human CD4+CD25+ regulatory T cells inhibit the differentiation of osteoclasts from peripheral blood mononuclear cells. Biochem Biophys Res Commun. 2007 Jun 15;357:1046–1052.

[76] Kong N, Lan Q, Su W, et al. Induced T regulatory cells suppress osteoclastogenesis and bone erosion in collagen-induced arthritis better than natural T regulatory cells. Ann Rheum Dis. 2012 Sep;71:1567–1572. published online Epub.

[77] Cha W, Fan R, Miao Y, et al. MicroRNAs as novel endogenous targets for regulation and therapeutic treatments. Medchemcomm. 2018 Mar 1;9:396–408.